

## Effective Masses of Electrons in Indium Arsenide and Indium Antimonide

R. J. SLADEK

*Westinghouse Research Laboratories, Pittsburgh 35, Pennsylvania*

(Received June 13, 1956)

Measurements of the electrical conductivity and Hall effect of *n*-type indium arsenide and indium antimonide specimens have been made between 1.5°K and 300°K. The dilute metallic character of these substances at low temperatures permits the Fermi level at absolute zero to be obtained from the electrical conductivity *versus* temperature data. From each Fermi level and the respective conduction electron concentration determined from the Hall effect, we obtained the following effective electron masses: InAs,  $m^*/m_0=0.020\pm 0.005$ ; and InSb,  $m^*/m_0=0.016\pm 0.007$ .

### I. INTRODUCTION

ACCORDING to the electron theory of metals, electrical conduction in a metal is due to quasi-free electrons in a band containing the Fermi level. For ordinary metals the concentration of these electrons is of the order of one per lattice atom and is independent of temperature, while the Fermi level is of the order of electron volts above the band edge and depends only slightly on temperature.

There are substances which are similar to what might be called dilute metals. They have fewer conduction electrons by orders of magnitude than an ordinary metal, and they have a degeneracy temperature that is below room temperature.

In the electron gas approximation, a simple expression relates the effective electron mass,  $m^*$ , to the concentration of conduction electrons,  $n$ , and the absolute zero Fermi level,  $\zeta_0$ . Thus if the latter two are known,  $m^*$  can be calculated.

For ordinary metals  $n$  is readily obtainable from electrical measurements (Hall effect), but more elaborate means are needed to determine  $\zeta_0$ , e.g., low-temperature heat capacity measurements.

For a dilute metal, temperatures both above and below the degeneracy temperature,  $T_D=\zeta_0/k$ , are accessible experimentally. By measuring the electrical conductivity in this temperature range and fitting a calculated conductivity curve to the data,  $\zeta_0$  can be determined under certain conditions as we shall see in Sec. II.

The dilute metal-like substances studied in this work are *n*-type InAs and *n*-type InSb. The effective electron mass in each of these substances will be determined from Hall effect and conductivity data in the extrinsic temperature range.

Electrical conductivity and Hall effect data between 1.5°K and 300°K were obtained for an *n*-type InAs sample and an *n*-type InSb sample. Data for another *n*-type InSb sample were taken from the work of Rollin and Petford.<sup>1</sup> The two InSb samples have different concentrations of (extrinsic) conduction electrons.

<sup>1</sup> B. V. Rollin and A. D. Petford, *J. Electronics* **1**, 171 (1955).

### II. METHOD

According to the theory of electrical conduction in a band of parabolic form, the electrical conductivity,  $\sigma$ , is given by the relation

$$\sigma \sim \int d\epsilon (-\epsilon \partial f_0 / \partial \epsilon) \epsilon^{\frac{1}{2}} \tau(\epsilon), \quad (1)$$

where  $\epsilon$  is the energy of the charge carrier,  $f_0$  is the Fermi function, and  $\tau(\epsilon)$  is the relaxation time, assumed to be a function of energy alone.

We shall assume that  $\tau(\epsilon)$  is independent of temperature and has the form

$$\tau \sim A \epsilon^{-\frac{1}{2}} + \epsilon^s, \quad (2)$$

where  $A$  and  $s$  will be determined by the best fit of (1) to the experimental data at temperatures where only extrinsic electrons are important for conduction.  $s$  is essentially equal to the slope of the experimental  $\log \sigma$  *versus*  $\log T$  plot at the high-temperature end of the range where scattering by ionized impurities is thought to be dominant. The reason for assuming  $\tau$  has the form indicated in Eq. (2) is to allow the data to be fitted with a form having some plausibility in terms of available theory for scattering by ionized impurities.<sup>2</sup>

For the  $\epsilon^{\frac{1}{2}}$  term in  $\tau$ , the integral in Eq. (1) can be evaluated directly, while for the  $\epsilon^s$  term this integral, which we denote by  $\sigma_2$ , can be expressed in terms of Fermi-Dirac functions.<sup>3</sup> Thus

$$\sigma_2 \sim F_{s+\frac{3}{2}}(\eta) / [F_{\frac{3}{2}}(\eta)]^{(2s+3)/3}, \quad (3)$$

where

$$F^t(\eta) \equiv \int_0^\infty \frac{x^t dx}{e^{x-\eta} + 1}.$$

Tables of  $F_t(\eta)$  are available for integral<sup>4</sup> and half-integral<sup>3,5</sup> values of  $t$ . To evaluate  $F_t(\eta)$  for values of  $t$

<sup>2</sup> E. Conwell and V. F. Weisskopf, *Phys. Rev.* **69**, 258 (1946); **77**, 388 (1950); V. A. Johnson and K. Lark-Horovitz, *Phys. Rev.* **71**, 374 (1947); H. Brooks, *Phys. Rev.* **83**, 879 (1951); R. B. Dingle, *Phil. Mag.* **46**, 831 (1955).

<sup>3</sup> J. MacDougall and E. C. Stoner, *Trans. Roy. Soc. (London)* **A237**, 67 (1938).

<sup>4</sup> P. Rhodes, *Proc. Roy. Soc. (London)* **A204**, 396 (1950).

<sup>5</sup> R. B. Dingle, see reference 2; and Beer, Chase, and Choquard, *Helv. Phys. Acta* **28**, 529 (1955).

for which  $F_t(\eta)$  is not tabulated, we have used numerical integration, series approximations,<sup>3,4</sup> or interpolation between  $F_t(\eta)/\Gamma(t+1)$  functions of different orders ( $t$  values), whichever was appropriate in each case.

Since we wish to calculate  $\sigma$  as a function of  $kT/\zeta_0$  while Eq. (3) gives  $\sigma_2$  in terms of  $\eta=\zeta/kT$ , with  $\zeta$  itself varying with temperature, we need to determine the value of  $\eta$  corresponding to each value chosen for  $kT/\zeta_0$ . This is done by using the fact that when the concentration of electrons in the conduction band is independent of temperature,  $F_{3/2}(\eta)=F_{3/2}(\eta_0)=\frac{2}{3}(\zeta_0/kT)^{3/2}$ . Thus  $\eta$  is determined from the value of the function  $F_{3/2}(\eta)$  at each value of  $kT/\zeta_0$ .

In order to determine  $A$  and the power  $s$  to be used for a given sample, a curve of  $\sigma$  versus  $kT/\zeta_0$  was obtained for each of several values of  $A$  and  $s$ . Each curve was then superposed on a log-log plot of the conductivity versus temperature data and was translated vertically and horizontally (as required) to see how well it could be made to fit the data. The best values of  $A$  and  $s$  to use were thus determined by trial and error.

The degeneracy temperature  $T_D=\zeta_0/k$  was determined from the optimum positioning of the curve of  $\sigma$  versus  $kT/\zeta_0$  as computed from the optimum  $A$  and  $s$ .

The effective electron mass was computed from the relation

$$m^* = \frac{1}{8} \left( \frac{3}{\pi} \right)^{1/3} \frac{\hbar^2 n^{2/3}}{\zeta_0}, \quad (4)$$

where  $n$ , the number of conduction electrons per cc, is obtained from the Hall coefficient,  $R_H$ , at lowest temperatures by the relation,

$$n = 1/R_H e c. \quad (5)$$

It should be noted that our method of obtaining  $m^*$  is applicable to semiconductors in which conduction is due to a constant number of charge carriers in a temperature range containing  $T_D$  and for which  $\tau$  is not an explicit function of temperature. However,  $\tau$  must vary rapidly enough with energy so that the electron mobility is strongly temperature-dependent, since this condition allows  $T_D$  and hence  $m^*$  to be determined with a minimum of ambiguity.

Our method assumes that there is a single conduction band responsible for the electrical properties. If there are several equivalent bands, it is necessary to divide the electron concentration,  $n$ , obtained using Eq. (5) by the number of equivalent bands.

### III. EXPERIMENTAL DETAILS

#### A. Specimens

Specimens approximately  $10 \times 2.5 \times 1$  mm were cut and lapped from polycrystalline  $n$ -type indium arsenide and single-crystal  $n$ -type indium antimonide. The indium arsenide was supplied by Dr. H. Welker of the

Siemens-Schuckertwerke Research Laboratory and the indium antimonide by Dr. S. Kurnick of the Chicago Midway Laboratories. Current and potential leads of No. 40 copper wire were attached to the specimens with tin or indium-tin solder. Both of these solders were used on InSb samples with either etched or lapped surfaces, and no difference in electrical properties was found at the selected temperatures where they were measured. A lapped surface and tin solder for contacts were used on the InAs specimen.

The specimens are identified in Table I.

#### B. Apparatus and Technique

Conventional low-temperature technique was used to obtain and measure the temperatures employed. For the Hall measurements, magnetic fields were provided by a large electromagnet or a solenoid and were measured with a rotating coil fluxmeter calibrated by proton resonance.

Specimen current, voltage drop, and Hall voltage, carbon resistance thermometer current and voltage, and thermocouple emf were measured by means of conventional dc potentiometric methods.

#### C. Errors

The scatter in our data on electrical conductivity and Hall effect versus temperature indicate an accuracy of  $\pm 5\%$  for  $\sigma$  and of  $\pm 12\%$  for  $R_H$ . Since the precision of our conductivity measurements, at any rate, is much better than this accuracy, inhomogeneities in the samples may be responsible for the scatter. The presence of inhomogeneities in the InAs sample was indicated by the fact that two separate sets of potential leads yielded

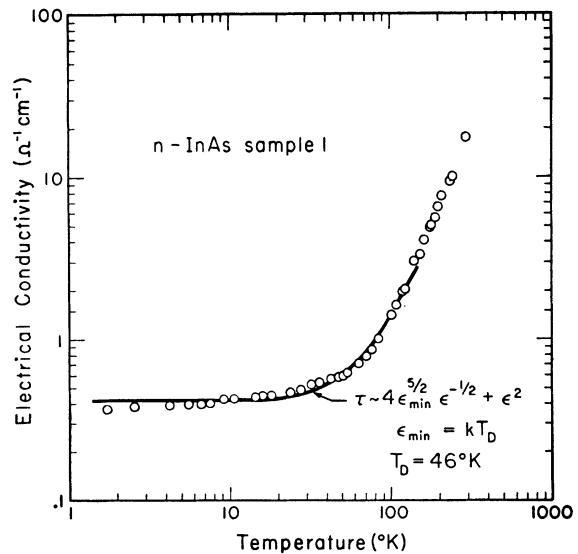


FIG. 1. Electrical conductivity versus temperature data (points) for InAs and the calculated conductivity curve for the extrinsic temperature range (solid line) obtained by using  $\tau \sim 4\epsilon_{\min}^{3/2}\epsilon^{-1/2} + \epsilon^2$ ,  $\epsilon_{\min} = \zeta_0 = kT_D$ ,  $T_D = 46^\circ\text{K}$ .

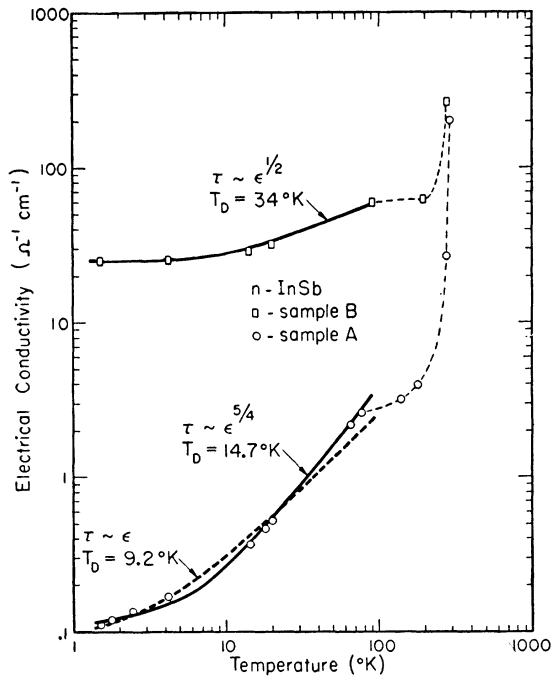


FIG. 2. Electrical conductivity *versus* temperature data (points) for InSb samples *A* and *B* and calculated conductivity curves. Solid curve drawn through sample *B* data is calculated by using  $\tau \sim \epsilon^1$ ,  $T_D = 34^\circ\text{K}$ . Solid curve for sample *A* is calculated by using  $\tau \sim \epsilon^{5/4}$ ,  $T_D = 14.7^\circ\text{K}$ . Dashed curve for sample *A* is calculated by using  $\tau \sim \epsilon$ ,  $T_D = 9.2^\circ\text{K}$ .

slightly different values for the conductivity at some, but not at all, temperatures.

#### IV. RESULTS

The electrical conductivity data are plotted *versus* absolute temperature in Figs. 1 and 2. Note that logarithmic scales are used. The data for sample *B* are taken from the work of Rollin and Petford.<sup>1</sup> The curves drawn in these figures are calculated and fitted to the data by the method outlined in Sec. II. Two curves are included for sample *A* to show the range of uncertainty in fitting a simple power law to the relaxation time. Clearly the power law which fits best depends on which experimental points are weighted most heavily in making the fit.

Hall coefficient *versus* temperature data are displayed in Fig. 3. For sample 1 we used a magnetic field of 3620 gauss, and for sample *A* a field of 300 gauss. In either case the magnetic field,  $H$ , was weak enough to satisfy the condition  $\mu H \ll 10^8$ , where  $\mu$  is the electron mobility at the lowest temperatures. However, for sample 1, this weak field criterion does not quite apply at the higher temperatures. ( $\mu H$  reaches a maximum of  $\sim 5 \times 10^7$  at  $200^\circ\text{K}$ .) For Hall measurements on sample *B*, Rollin and Petford<sup>1</sup> used a field of 6000 gauss. Since the mobility of their sample was greater than 43 000  $\text{cm}^2/\text{v sec}$  at all temperatures reported, we can expect that they have reached the region in which  $R_H$  is

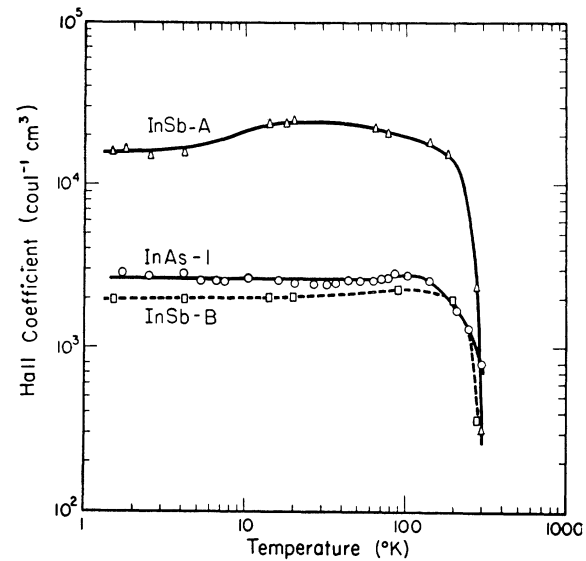


FIG. 3. Hall coefficient as a function of absolute temperature for indium arsenide and indium antimonide samples. See text for magnetic fields used for measurements.

independent of magnetic field strength. Thus for their sample Eq. (5) can be used directly to obtain charge carrier concentration throughout the extrinsic temperature range.

Table I gives a summary of the quantitative results deduced from the conductivity and Hall effect measurements. The conduction band degeneracy temperature,  $T_D$  was obtained from the calculated curve fitted to the conductivity data in each case. For sample *A* we take  $T_D$  to be almost that obtained from the curve calculated for  $\tau \sim \epsilon^{5/4}$ . The concentration of extrinsic electrons,  $n$ , was calculated from the Hall coefficient at lowest temperatures.<sup>6</sup> Utilizing the tabulated values of  $T_D$  and  $n$ , we obtain the effective mass ratios listed in the last column of Table I. The indicated errors for  $m^*/m_0$  are estimated from the possibility of alternative calculated curves fitting the conductivity data.

TABLE I. Results obtained from electrical conductivity and Hall effect measurements for InAs and InSb samples.

Sample	Material	$n$ , $\text{cc}^{-1}$	$T_D$ , $^\circ\text{K}$	$m^*/m_0$
1	InAs	$3.0 \times 10^{15}$	46	$0.020 \pm 0.005$
<i>A</i>	InSb	$3.9 \times 10^{14}$	14	$0.016 \pm 0.007$
<i>B</i> <sup>a</sup>	InSb	$3.1 \times 10^{15}$	34	$0.026 \pm 0.007$

<sup>a</sup> Data from Rollin and Petford, reference 1.

#### V. DISCUSSION

##### A. Electrical Conductivity

The temperature dependence of the electrical conductivity of InAs, presented in Fig. 1, can be understood

<sup>6</sup> Since  $R_H$  for the InAs sample was somewhat field-dependent at 3620 gauss, we measured it up to 26 000 gauss at  $4.2^\circ\text{K}$ .  $R_H$  reached a constant value above 10 000 gauss, so we used this value to compute  $n$ .

as follows. The increase in  $\sigma$  with  $T$  up to 140°K is due to increasing electron mobility since the constancy of the Hall coefficient in this temperature range (see Fig. 3) indicates no change in the concentration of electrons with temperature. We note that an increasing electron mobility is in qualitative agreement with that predicted by theory when scattering by ionized impurities is dominant.

The continued increase in  $\sigma$  with  $T$  for InAs above 140°K is due to an increased concentration of conduction electrons. Thus, we must limit our curve fitting for InAs to the temperature range below 140°K.

The relaxation time for best quantitative fit to our conductivity results for InAs below 140°K is as indicated in Fig. 1.

At lowest temperatures the measured conductivity of InAs retains some slight temperature dependence which cannot be fitted by the same relaxation time which fits the data at higher temperatures. Multiplying each measured value of the conductivity by the respective value measured for the Hall coefficient removes most of this temperature dependence in the Hall mobility indicating that perhaps there is a very slight decrease in carrier concentration as the temperature is lowered.

For the InSb samples, the increase in  $\sigma$  with  $T$  up to 80°K is due to an increasing electron mobility, as would be expected for scattering predominantly by ionized impurities. A single-term relaxation time proportional to a small positive power of the energy is adequate to fit the data in this temperature range (see Fig. 2).

Above 80°K scattering by lattice waves becomes important in the InSb samples, so we have limited our analysis to the temperature interval below 80°K.

It may be noted that the mobility of InSb-*A* is smaller than that of InSb-*B* at lowest temperatures. This we believe is due to the total impurity content of sample *A* being comparable to that of sample *B* although the electron concentration is much smaller in the former. Thus sample *A*, at any rate, would seem to be highly compensated, although still very pure chemically (say less than 1 part per million). The different temperature dependences of the mobilities in the InSb samples is due to the different degeneracy temperatures of the two samples.

### B. Hall Effect

The relatively flat portion of the  $R_H$  versus  $T$  curve for each sample (see Fig. 3) indicates the temperature range in which the concentration of electrons is independent of temperature. These electrons presumably come from excess donor atoms. The sharp drop in  $R_H$  at temperatures above 150°K for each of the specimens is due to the presence of intrinsic electrons in the conduction band which have been thermally excited from the valence band.

When the conduction band is not statistically degenerate, a temperature-dependent numerical factor must be included in the right-hand side of Eq. (5) when  $R_H$  is not saturated by the magnetic field used. This factor depends on the scattering mechanism and can be calculated when the functional form of  $\tau$  is known. For sample *A*, using the  $\tau$  which fits the conductivity data, we find that this factor will account approximately for the broad maximum in the experimental  $R_H$  versus  $T$  plot.

No maximum occurs in the Hall coefficient of our InAs sample although one might be expected in view of the above remarks. We attribute this to the increase in  $\mu H$  with temperature causing  $R_{H=3620}/R_{H\rightarrow 0}$  to decrease as the temperature is increased.

### C. Effective Masses

The two values obtained for the effective electron mass in InSb agree with each other to within experimental error. This is in accord with the curvature of the conduction band being constant as is assumed in the electron gas approximation utilized in this paper. In addition, these values are in reasonable agreement with the value for the effective mass obtained from cyclotron resonance ( $0.013 \pm 0.001m_0$ ),<sup>7</sup> and the values obtained from thermoelectric power measurements ( $0.014m_0$ <sup>8</sup> and  $0.037m_0$ <sup>9</sup>).

The value of the effective electron mass we have obtained for InAs is somewhat smaller than those obtained by other methods,  $0.055m_0$  from infrared absorption edge data<sup>10</sup> and  $0.064$  from thermoelectric power measurements in the intrinsic temperature range.<sup>9</sup> However, it should be noted that for InSb, thermoelectric power measurements below the intrinsic range yielded the smaller of the values for  $m^*$  quoted above. This value is only about one-third of the value obtained in the intrinsic temperature range.

In view of the above remarks, thermoelectric power measurements on *n*-type InAs below the intrinsic temperature range would seem desirable. It will be interesting to see what value cyclotron resonance will yield for the effective mass of electrons in InAs.

## VI. CONCLUSIONS

The concept of a dilute metal and the electron gas approximation allow determination of the effective masses of electrons in *n*-type InAs and InSb from electrical conductivity and Hall effect measurements. For InAs we found  $m^*=0.020m_0$ , and for InSb we found  $m^*=0.016m_0$ .

<sup>7</sup> Dresselhaus, Kip, Kittel, and Wagoner, Phys. Rev. **98**, 556 (1955).

<sup>8</sup> H. P. R. Frederikse and E. V. Mielczarek, Phys. Rev. **99**, 1889 (1955).

<sup>9</sup> H. Weiss, Z. Naturforsch. **11a**, 131 (1956).

<sup>10</sup> F. Stern and R. M. Talley, Phys. Rev. **100**, 1638 (1955).

The low-temperature electrical properties of  $n$ -type InAs, measured for the first time in this work, suggest that a pure enough sample of this material should exhibit the electron localization effect in the presence of a strong magnetic field which has been discovered in  $n$ -type InSb (sample A).<sup>11</sup>

<sup>11</sup> R. W. Keyes and R. J. Sladek, Phys. Rev. **100**, 1262 (A) (1955).

## VII. ACKNOWLEDGMENTS

The stimulating interest of Dr. R. W. Keyes in this work is gratefully acknowledged. Thanks are due to Dr. E. N. Adams for advice and for reading and criticizing the manuscript.

We are indebted to Dr. H. Welker of the Siemens-Schuckertwerke Research Laboratory and to Dr. S. Kurhick of the Chicago Midway Laboratories for providing the material for the samples.

## Sodium Nuclear Quadrupole Interactions in $\text{NaClO}_3$ and $\text{NaBrO}_3$ <sup>†</sup>

H. S. GUTOWSKY AND G. A. WILLIAMS\*  
*Noyes Chemical Laboratory, University of Illinois, Urbana, Illinois*  
 (Received October 8, 1956)

The electric quadrupole splitting of the  $\text{Na}^{23}$  nuclear magnetic resonance has been measured in single crystals as a function of pressure and of temperature for  $\text{NaClO}_3$  and as a function of pressure for  $\text{NaBrO}_3$ . The values for  $(1/P)\Delta\nu/\nu$  are  $+7.7 \times 10^{-6}$  and  $+6.0 \times 10^{-6} \text{ kg}^{-1} \text{ cm}^2$ , respectively, and for  $(1/T)\Delta\nu/\nu$ ,  $-4.2 \times 10^{-4} \text{ deg}^{-1}$ . The results suggest that the temperature and pressure dependence of the sodium coupling results mainly from the change with volume of the crystalline field, which also makes an appreciable contribution to the temperature dependence of the chlorine coupling.  $e^2qQ/h$  for sodium is found to be  $779.2 \pm 4 \text{ kc/sec}$  in  $\text{NaClO}_3$  and  $842.4 \pm 4 \text{ kc/sec}$  in  $\text{NaBrO}_3$ . In  $\text{NaClO}_3$  the electric field gradient at the sodium nuclei varies with volume approximately as  $V^{-2}$  indicating the importance of other than simple Coulombic effects.

### I. INTRODUCTION

SEVERAL earlier investigations of nuclear electric quadrupole interactions in crystals are particularly pertinent to the present study. Wang *et al.*<sup>1</sup> found the  $\text{Cl}^{35}$  pure quadrupole resonance frequency in  $\text{NaClO}_3$  to be 29.920 Mc/sec at 26°C; the temperature coefficient of the frequency has also been measured<sup>2</sup> and corresponds to  $(1/T)\Delta\nu/\nu = -1.4 \times 10^{-4} \text{ deg}^{-1}$ . There have been several studies of the effects of hydrostatic pressure, at room temperature, on the  $\text{Cl}^{35}$  quadrupole resonance. Livingston<sup>3</sup> has given a value of  $+0.91 \times 10^{-6} \text{ kg}^{-1} \text{ cm}^2$  for  $(1/P)\Delta\nu/\nu$  in  $\text{KClO}_3$  and states that the results for  $\text{NaClO}_3$  are very similar. This is confirmed by specific values of  $+0.93 \times 10^{-6}$  and  $(0.93 \pm 0.01) \times 10^{-6} \text{ kg}^{-1} \text{ cm}^2$  obtained for  $\text{NaClO}_3$  by Wang<sup>2</sup> and by Benedek, Bloembergen, and Kushida.<sup>4</sup> In addition, the pressure dependence of the chlorine pure quadrupole resonance in  $p$ -dichlorobenzene has been measured by Dautreppe and Dreyfus.<sup>5</sup> In all cases, the frequencies increase with pressure.

<sup>†</sup> Assisted by the Office of Naval Research.

\* Now at Department of Physics, Stanford University, Stanford, California.

<sup>1</sup> Wang, Townes, Schawlow, and Holden, Phys. Rev. **86**, 809 (1952).

<sup>2</sup> T. C. Wang, Ph.D. thesis, Columbia University, 1955 (unpublished).

<sup>3</sup> R. Livingston (private communication).

<sup>4</sup> Benedek, Bloembergen, and Kushida, Bull. Am. Phys. Soc. Ser. II, **1**, 11 (1956).

<sup>5</sup> D. Dautreppe and B. Dreyfus, Compt. rend. **241**, 795 (1955).

The pressure dependence of the chlorine quadrupole coupling in  $p$ -dichlorobenzene was ascribed<sup>6</sup> to an increase in the frequencies of the molecular torsional oscillations. Such thermal vibrations were proposed earlier<sup>6,7</sup> as the sole mechanism which decreases the coupling upon increasing temperature in molecular crystals. The oscillations average out part of the electric field gradients and reduce the quadrupole coupling by an amount proportional to the mean square displacements. The latter increase with temperature, and decrease with increasing frequency of oscillation and thus with pressure. This model accounts qualitatively for the observations. However, the temperature dependences calculated with the model appear to be invariably smaller than those found experimentally,<sup>8-10</sup> particularly at higher temperatures. It has been suggested<sup>9</sup> that this apparent discrepancy results from the temperature dependence of the oscillational frequencies, at least for  $p$ -dichlorobenzene and  $p$ -dibromobenzene.

There is also the possibility that some of the effects arise from the contributions of the crystalline field to the field gradients. This contribution would be inversely proportional to the molar volume of the sample and would respond qualitatively to temperature and pres-

<sup>6</sup> H. G. Dehmelt and H. Krüger, Z. Physik **129**, 401 (1951).

<sup>7</sup> H. Bayer, Z. Physik **130**, 227 (1951).

<sup>8</sup> D. W. McCall, Ph.D. thesis, University of Illinois, 1953 (unpublished).

<sup>9</sup> B. Dreyfus and D. Dautreppe, Compt. rend. **239**, 1618 (1954).

<sup>10</sup> T. C. Wang, Phys. Rev. **99**, 566 (1955).